VIP Nanostructures

DOI: 10.1002/anie.200905245

Etching and Dimerization: A Simple and Versatile Route to Dimers of Silver Nanospheres with a Range of Sizes**

*Weiyang Li, Pedro H. C. Camargo, Leslie Au, Qiang Zhang, Matthew Rycenga, and Younan Xia**

Silver nanostructures have attracted considerable interest because of their spectacular property known as surface plasmon resonance (SPR), which has enabled their widespread use as optical probes, contrast agents, sensors, plasmonic waveguides, and substrates for surface-enhanced Raman scattering (SERS).[1] SERS is an application of particular interest owing to its use in ultrasensitive trace analysis and single-molecule detection, which have been demonstrated with samples fabricated from Ag nanoparticles through salt-induced aggregation.[2] For these substrates, it is generally accepted that single-molecule sensitivity is only possible at a specific site known as the hot spot—the gap region between a pair of strongly coupled Ag (or Au) nanoparticles, where the electromagnetic field can be amplified dramatically. This amplification leads to the observation of enhancement factors (EFs) several orders of magnitude greater than those of the individual nanoparticles.[3]

Although a tremendous amount of effort has been directed to the study of the hot-spot phenomenon, it remains elusive and poorly understood. One of the most commonly used methods for generating hot spots is based on the salt-induced, random aggregation of Ag or Au colloidal particles in a solution phase.[4] Besides the poor reproducibility that is characteristic of a random aggregation process in terms of interparticle spacing and numbers of particles, there is also the problem of the irregularity and nonuniformity of the constituent nanoparticles in terms of size, shape, crystallinity, and overall morphology. As a result, it has been hard (if not impossible) to correlate the observed giant EF to the specific attribute(s) of a hot spot.

In an attempt to address this issue, many research groups have developed various methods for controlling the assembly of Ag or Au nanoparticles into well-defined structures for SERS applications.[5] Most of these studies, however, require functionalization of the surface of the nanoparticles with organic or biological molecules.[6] The structures fabricated by using these methods are actually not suitable for SERS-based detection because the organic or biological linkers bridging the two adjacent nanoparticles tend to prevent the analyte molecules from entering the hot-spot region. More recently, our research group reported the synthesis of dimers consisting of single-crystal Ag spheres with a diameter of less than 30 nm on the basis of the polyol synthesis, whereby the growth and dimerization of Ag nanospheres could be promoted at the same time by adding a small amount of NaCl to the reaction solution.[7] However, this growth-based method cannot be extended to the production of dimers of Ag spheres larger than 30 nm in diameter because further growth would lead to the transformation of the spheres into cubic particles. In our previous SERS study on individual dimers of 30 nm Ag spheres, the SERS signals were very weak as a result of the relatively small size of the spheres and the small number of molecules trapped in the hot-spot region.[7] No SERS signals were detected for individual Ag nanospheres of the same size that were studied for comparison. Thus, dimers with such a small size present limitations for SERS studies. It would be a great advantage to have dimers composed of Ag nanospheres with a broad range of sizes for SERS studies owing to the simplicity of spherical particles for computational simulation.

Our research group has developed a number of procedures for the production of Ag nanocubes. The edge lengths of the nanocubes could be controlled from 30 to 200 nm by adjusting the reaction parameters.[8] Herein we demonstrate a facile method based upon wet etching with $Fe(NO_3)_3$ for the generation of well-defined dimers of Ag nanospheres from a uniform sample of Ag nanocubes. The etching reaction was performed at room temperature in ethanol with the help of poly(vinyl pyrrolidone) (PVP). When an aqueous suspension of Ag nanocubes was mixed with a small amount of an aqueous solution of $Fe(NO_3)_3$ in ethanol, the corners and edges of the cubes were truncated to form spheres, which were also induced to dimerize in the same reaction mixture. This approach was found to work well for Ag cubes with edge lengths in the range of 40–100 nm.

The procedure we used to fabricate the dimers is illustrated schematically in Figure 1. We started with Ag nanocubes dispersed in a mixture of ethanol (major component) and water. According to our previous studies, an aqueous solution of $Fe(NO_3)_3$ can be used as a powerful wet etchant to dissolve Ag[9] according to Equation (1):

$$Ag(s) + Fe(NO_3)_3(aq) \rightarrow AgNO_3(aq) + Fe(NO_3)_2(aq) \quad (1)$$

It is well-known that the stability of a colloidal system is

[*] W. Li, P. H. C. Camargo, L. Au, Q. Zhang, M. Rycenga, Prof. Y. Xia
Department of Biomedical Engineering
Washington University
Saint Louis, MO 63130 (USA)
E-mail: xia@biomed.wustl.edu

[**] This research was supported in part by a research grant from the NSF (DMR-0804088) and a 2006 Director's Pioneer Award from the NIH (DP1 OD000798). P.H.C.C. was also supported in part by the Fulbright Program and the Brazilian Ministry of Education (CAPES). Part of the study was performed at the Nano Research Facility (NRF), a member of the National Nanotechnology Infrastructure Network (NNIN), which is supported by the NSF under ECS-0335765. NRF is part of the School of Engineering and Applied Science at Washington University in St. Louis.

Supporting information for this article is available on the WWW under http://dx.doi.org/10.1002/anie.200905245.

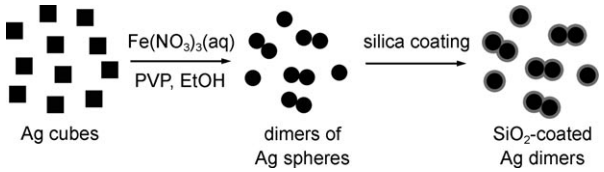

Figure 1. Schematic representation of the formation of dimers of Ag nanospheres during the etching of Ag nanocubes with an aqueous solution of $Fe(NO_3)_3$ in ethanol.

dependent on the concentration of electrolytes or ionic species in the medium.[7,10] According to the Derjaguin–Landau–Verwey–Overbeek (DLVO) theory, an increase in the electrolyte concentration will decrease the stability of a colloidal system and result in dimerization as well as higher degrees of agglomeration of the colloidal particles. Therefore, when a small amount of an aqueous solution of $Fe(NO_3)_3$ was added to a suspension of Ag nanocubes in ethanol, the salt not only served as an etchant for the Ag cubes but also triggered the resultant Ag spheres to dimerize. The reaction was typically performed in a medium containing a large amount of ethanol, a small quantity of water, and a certain amount of PVP. Both PVP and ethanol played an important role in the dimerization process for reasons to be explained later. To confirm that the dimers were indeed formed in the solution phase rather than on the substrate during the preparation of SEM or TEM samples, we added tetraethylorthosilicate (TEOS) to the reaction mixture to fix the dimers through silica coating.

Figure 2 A,B shows typical SEM and TEM images of Ag nanosphere dimers prepared from Ag nanocubes with edge lengths of approximately 100 nm (see Figure S1 in the Supporting Information). White and black ellipses were drawn to highlight the dimers in the SEM and TEM images, respectively. The large number of dimers distributed over a wide area of the substrate indicates that a significant proportion of the particles in the final product existed in the well-defined dimeric structure. We counted over 150 Ag nanoparticles on the SEM and TEM images and concluded that the percentage of dimerization (i.e., the number of dimerized spheres divided by the total number of spheres) was approximately 66 %. Magnified SEM and TEM images of the dimers (insets in Figure 2 A,B) suggested that the dimers had a smooth surface. The magnified TEM image of an individual dimer clearly shows the spherical shape of the two constituent Ag spheres, which had diameters of 79.4 and 81.1 nm. Since the cubes we used for the etching process were single crystals, the resulting nanospheres in the dimers were also single crystals, as confirmed by the uniform contrast observed across each particle by TEM and further supported by the high-resolution TEM image shown in Figure 2 C. A narrow gap approximately 0.67 nm wide between the two nanospheres formed the so-called hot-spot region. Figure 2 D shows a TEM image of the sample after silica coating. Again, a large number of dimers can be readily identified in this sample. This result demonstrates clearly that the dimers were formed in the reaction solution rather than on the substrate during the preparation of the SEM and TEM samples. The strong contrast difference between Ag and SiO_2 in a magnified TEM image of an individual silica-coated dimer (Figure 2 D) suggests that the SiO_2 coating had a more or less uniform thickness of approximately 11.6 nm over the entire surface of the dimer.

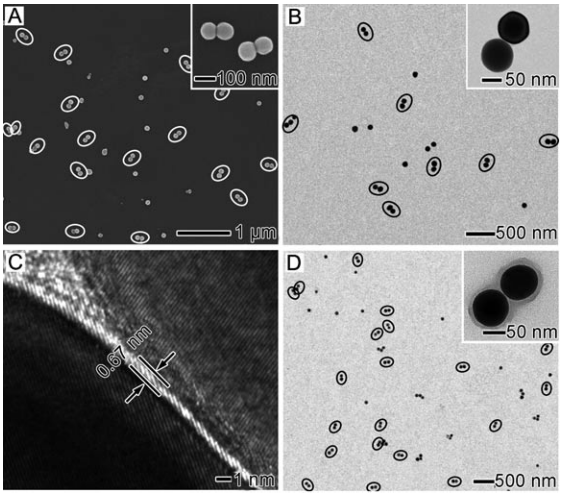

Figure 2. A) SEM and B) TEM images of Ag nanosphere dimers prepared from 100 nm Ag nanocubes. C) High-resolution TEM image of the gap in a dimer and D) TEM image of dimers after the coating of their surface with silica. The dimers are highlighted by white and black ellipses in the SEM and TEM images, respectively. The inset in each image shows a magnified SEM or TEM image of the same sample. Experimental conditions: PVP (0.01 g), ethanol (1.5 mL), aqueous $Fe(NO_3)_3$ solution (10 mM, 50 μL), etching for 2 h at room temperature.

This etching method for the preparation of dimers can be extended to Ag nanospheres with a range of different sizes by using Ag nanocubes with different edge lengths as precursors. Figure 3 A,B shows typical SEM and TEM images of Ag nanosphere dimers derived from Ag cubes with edge lengths of approximately 82 nm (see Figure S1 in the Supporting Information). Figure 3 C,D shows SEM and TEM images of dimers fabricated from Ag cubes with edge lengths of approximately 47 nm (see Figure S1 in the Supporting Information). As in the case of the dimers shown in Figure 2, a large number of dimers, highlighted again by white and black ellipses, can be identified readily in the SEM and TEM images. The inset in each image shows a magnified SEM or TEM image of the sample. These magnified images indicate that all spheres had a smooth surface and exhibited a round profile. The dimers derived from Ag cubes with diameters of 82 and 47 nm were composed of single-crystal spheres of approximately 63 and 40 nm in diameter, respectively. Table 1 provides a summary of the major parameters for the different samples. The as-prepared samples all had relatively high percentages of dimerization (> 60 %), and the gap widths of the dimers all fell into the narrow range of 0.6–0.7 nm.

UV/Vis extinction spectra were recorded for the cube precursors and the resulting dimers (see Figure S2 in the Supporting Information). Four SPR peaks were present for both the 100 and the 82 nm cubes, whereas three peaks could be resolved for the 47 nm cubes. These observations are consistent with the characteristic dipole and quadrupole

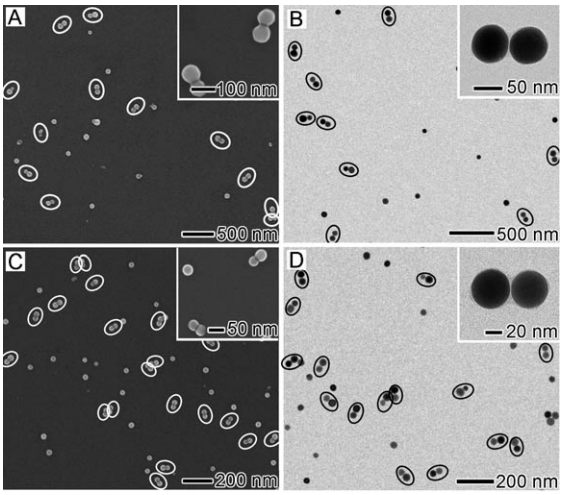

Figure 3. A) SEM and B) TEM images of Ag nanosphere dimers prepared from 82 nm Ag nanocubes. C) SEM and D) TEM images of Ag nanosphere dimers prepared from 47 nm Ag nanocubes. The dimers are highlighted by white and black ellipses in the SEM and TEM images, respectively. The inset in each image shows a magnified SEM or TEM image of the same sample. The dimer composed of 63 nm nanospheres was prepared from 82 nm Ag nanocubes under the conditions described in Figure 2. The dimer composed of 40 nm nanospheres was prepared from 47 nm Ag nanocubes by the addition of aqueous $Fe(NO_3)_3$ (10 mM, 40 μL) with an etching time of 1 h.

Table 1: A summary of the edge length of the Ag nanocubes (l_{cube}), the diameter of the resultant spheres in the dimers after etching (d_{sphere}), the percentage of dimerization, and the width of the gap region in the dimer.

l_{cube} [nm]	d_{sphere} [nm]	Dimerization [%]	Gap width [nm]
100.4 ± 4.5	80.4 ± 4.2	66	0.67
82.2 ± 4.5	63.0 ± 3.7	65	0.69
47.4 ± 3.5	39.7 ± 3.4	61	0.65

resonances for Ag nanocubes of these sizes.[11] After wet etching and dimerization, the primary SPR peak of the samples were all blue-shifted because of the decrease in size with respect to the corresponding cube precursors. The two peaks located at 350 and 390 nm disappeared as a result of the higher symmetry of a sphere relative to that of a cube. A shoulder peak that appeared at approximately 500 nm (just next to the primary SPR peak) for the 40 nm Ag sphere dimers is indicative of dimerization. This result is consistent with our previous SPR study on dimers composed of 30 nm Ag spheres.[7] However, the existence of a shoulder peak that would imply dimerization could not be resolved from the spectra of dimers composed of 80 and 63 nm spheres. The broad SPR peaks observed for Ag spheres of such large sizes may overshadow the shoulder peaks characteristic of dimers.

Interestingly, we found that PVP played an important role in the formation of dimers of Ag spheres. The etching reaction did not proceed without the addition of PVP. Figure 4A shows an SEM image of the product obtained under similar experimental conditions to those used for the sample shown in Figure 2 but without PVP. In this case, the product exhibited a cubic shape instead of the spherical morphology, and no dimers were found. The surface of the cubes shown in Figure 4A was much rougher than that of the precursor cubes,

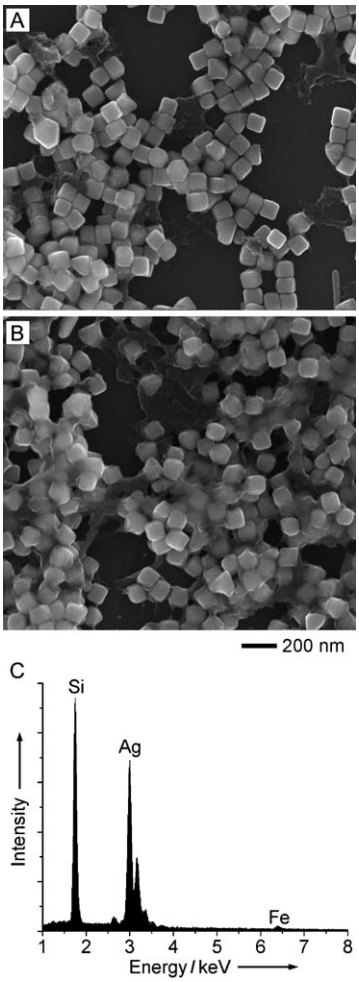

Figure 4. A,B) SEM images of two samples obtained by wet etching for 2 and 18 h, respectively. The etching was carried out under similar conditions to those described in Figure 2, but without the addition of PVP. C) EDX spectrum of the sample in (B).

and it was evident that a coating had been deposited on the surface. When the reaction time was extended to 18 h, more of this coating was found on the surface of the resulting cubes, and still no dimers were observed (Figure 4B). Thus, it appeared that the etching process was essentially blocked by the coated material. We performed energy-dispersive X-ray (EDX) analysis to identify the composition of the coating on the surface of the nanocubes (Figure 4C). Besides a peak for Si from the substrate and a peak for Ag from the cubes, we also detected a peak for Fe. It is known that Fe^{III} ions tend to undergo hydrolysis in an aqueous solution to form iron hydroxide, $Fe(OH)_3$, according to Equation (2):

$$Fe^{3+} + 3\,H_2O \rightleftharpoons Fe(OH)_3 + 3\,H^+ \qquad (2)$$

Even though the etching process was performed in a medium largely composed of ethanol, a small amount of water was introduced into the system when we added the aqueous $Fe(NO_3)_3$ solution (40 or 50 μL) and the aqueous suspension of Ag nanocubes (20 μL). Therefore, the formation of $Fe(OH)_3$ during the etching process was inevitable. Furthermore, $Fe(OH)_3$ has long been known to be a good

adsorbent and is widely used in water purification for entrapping and removing contaminants. Thus, it can readily adsorb onto the surface of Ag nanocubes. We found previously that PVP interacted strongly with the surface of Ag nanoparticles, with preferential adsorption on the {100} facets.[12] Since the surface of the Ag cubes is covered by {100} facets, it is possible that PVP can prevent the adsorption of $Fe(OH)_3$ onto the surface of the cubes to thereby facilitate the etching process. Ethanol was also found to be a key component for the successful preparation of the dimers. No dimers were observed in our previously reported study in which the etching was performed in water, even with the addition of PVP.[9b] A coating, most likely $Fe(OH)_3$, was also observed on the surface of the product prepared in water. As Fe^{III} ions are hydrolyzed much more rapidly in water than in ethanol, it is not unexpected that considerably more $Fe(OH)_3$ would be formed when the reaction was performed in water. The $Fe(OH)_3$ coating would have then impeded the formation of dimers.

We performed SERS measurements on the dimers of Ag nanospheres with various sizes. We used 4-methylbenzenethiol (4-MBT) as the probe molecule because it is known to form a well-defined monolayer on the Ag surface with a characteristic molecular footprint, which is needed to enable estimation of the total number of molecules probed in the SERS measurement and thus calculation of the enhancement factor (EF). Furthermore, the relatively small size of 4-MBT molecules makes it easier for them to get into the hot-spot region of the dimers. SERS spectra were recorded for a single dimer composed of 80 nm Ag spheres with the laser polarized parallel (Figure 5, top trace) and perpendicular (middle trace) to the long axis of the dimer. The bottom trace in Figure 5 is the SERS spectrum recorded for an individual Ag nanosphere. The two strong peaks at 1072 and 1583 cm^{-1} are the characteristic peaks for 4-MBT. The peak at 1072 cm^{-1} is due to a combination of the phenyl ring-breathing mode, CH in-plane bending, and CS stretching, and the peak at 1583 cm^{-1} can be assigned to the phenyl ring-stretching motion (8a vibrational mode).[13] The broad band observed in the middle and bottom trace at 900–1000 cm^{-1} originated from the Si substrate. To facilitate comparison of the SERS spectra for the three different systems, we amplified the SERS signals in the middle and bottom spectra by a factor of 10. It is clear that the intensity of the characteristic 4-MBT SERS peaks decreased in the following order: dimer (parallel) $\gg$ dimer (perpendicular) $>$ single sphere.

We used the peak at 1583 cm^{-1} (the strongest band in the spectra) to estimate the EF according to Equation (3):

$$EF = (I_{SERS}\, N_{bulk})/(I_{bulk}\, N_{SERS}) \quad (3)$$

in which I_{SERS} and I_{bulk} are the intensities of the same band in the SERS and normal Raman spectra, N_{bulk} is the number of molecules probed for a bulk sample, and N_{SERS} is the number of molecules probed in the SERS spectrum. The intensities I_{SERS} and I_{bulk} were determined from the area of the 1583 cm^{-1} band. N_{bulk} was calculated on the basis of the Raman spectrum of an 0.1 M 4-MBT solution in 12 M aqueous NaOH and the focal volume of our Raman system (1.48 pL). N_{SERS} was determined according to the assumption that a monolayer of 4-MBT molecules was formed on the Ag surface with a molecular footprint of 0.19 nm^2.[14] The N_{SERS} value is a theoretical maximum number of molecules. Therefore, the actual EF is believed to be higher than the value reported herein.

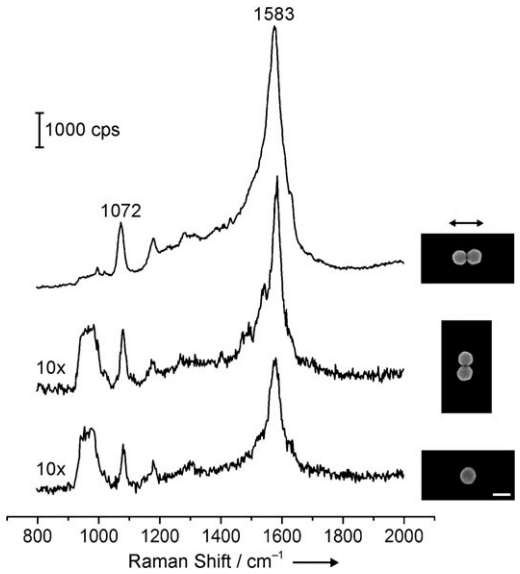

Figure 5. SERS spectra recorded for a dimer of Ag nanospheres with the laser polarization parallel (top trace) and perpendicular (middle trace) to the longitudinal axis of the dimer, and for a single Ag nanosphere (bottom trace). As indicated by "10×", the intensity of the SERS signals was multiplied by a factor of 10 for the middle and bottom traces. The insets show the corresponding SEM images. The scale bar corresponds to 100 nm and is applicable to all images. cps = counts per second.

Table 2 summarizes the EFs for dimers of Ag nanospheres with three different sizes, with the laser polarization parallel and perpendicular to the long axis of the dimer, as well as the EFs of the corresponding individual spheres. The EFs for the dimer decreased with decreasing size of the spheres. Furthermore, the EFs for dimers with laser polarization parallel to the long axis of the dimer are all much higher than the corresponding EFs with the polarization perpendicular to the long axis of the dimer. This result indicates that the SERS signals for the dimer were polarization dependent, which is consistent with our previous study on dimers composed of 30 nm Ag spheres.[7] The strong dependence on laser polarization could be attributed to the difference in electric-field enhancement in different excitation directions.[15] The EF of an individual sphere was much lower than that of the corresponding dimer. This difference is an indication of the hot-spot phenomenon. Furthermore, the EF (1.7×10^8) for a

Table 2: Enhancement factors (EFs) for dimers of Ag nanospheres with the laser polarization parallel ($EF_{dimer,parallel}$) and perpendicular ($EF_{dimer,perp.}$) to the longitudinal axis of the dimer, and for the corresponding spheres (EF_{sphere}).

d_{sphere} [nm]	$EF_{dimer,parallel}$	$EF_{dimer,perp.}$	EF_{sphere}
80.4 ± 4.2	1.7×10^8	1.5×10^7	1.0×10^7
63.0 ± 3.7	9.3×10^7	9.2×10^6	7.8×10^6
39.7 ± 3.4	3.9×10^7	4.6×10^6	1.2×10^6

dimer of 80 nm spheres with laser polarization parallel to the long axis of the dimer is almost 10 times higher than that observed previously for a dimer of 30 nm spheres.[7]

In summary, we have prepared well-defined dimers composed of Ag spheres by etching Ag nanocubes of various sizes. This method can be extended to the production of dimers of Ag nanospheres with a wide range of sizes and thus opens the door for experimental studies on the hot-spot phenomenon in SERS. With 4-MBT as a probe molecule, a SERS EF on the order of 1.7×10^8 was measured for an individual dimer consisting of 80 nm spheres. We believe that these well-defined dimers are attractive for various applications, including single-molecule detection, plasmonics, sensing, and imaging contrast enhancement.

Experimental Section

The protocols for silver-nanocube synthesis have been reported in detail elsewhere. The 47 nm cubes were synthesized by a sulfide-mediated polyol synthesis.[8b] The 82 and 100 nm cubes were prepared by a HCl-mediated polyol synthesis that involved oxidative etching of twinned seeds.[8a] In a typical synthesis of dimers of Ag nanospheres, PVP (0.01 g; Aldrich, $M_w \approx 55\,000$, 04207JD) was dissolved in ethanol (1.5 mL), and a small aliquot of Ag nanocubes (dispersed in water, 20 μL) was added to this solution. Under magnetic stirring, the nanocube suspension was mixed with an aqueous solution of $Fe(NO_3)_3$ (10 mM, 50 μL; Aldrich, 05713 KH), and the resulting mixture was stirred at room temperature for 2 h. The product was then collected by centrifugation at 10000 rpm for 5 min and washed three times with ethanol. (To prepare the dimer of 40 nm spheres, aqueous $Fe(NO_3)_3$ (10 mM, 40 μL) was added, and the etching time was 1 h.) The sample was then redispersed in ethanol for further characterization.

In a typical procedure for the silica coating of dimers of Ag nanospheres, the as-prepared dimers were mixed with ethanol (0.5 mL), and a portion of this mixture (0.25 mL) was transferred to a mixture of ethanol (0.8 mL) and deionized water (20 μL). Under continuous magnetic stirring, a 29% ammonia solution (20 μL) and TEOS (10 μL; Aldrich, 09118DJ) were added sequentially, and the resulting mixture was stirred at room temperature for 5 h. The mixture was then centrifuged at 10000 rpm to isolate the precipitate, which was then redispersed in ethanol for further characterization.

TEM images were captured by using a Tenai G2 Spirit Twin microscope operated at 120 kV (FEI, Hillsboro, OR). High-resolution TEM images were captured by using a field-emission 2100F microscope (JEOL, Tokyo, Japan) operated at 200 kV. SEM images were captured by using a Nova NanoSEM 230 field-emission microscope (FEI, Hillsboro, OR) operated at an accelerating voltage of 15 kV. Samples were prepared by dropping a suspension of the particles in ethanol on a piece of silicon wafer (for SEM) or carbon-coated copper grid (for TEM). UV/Vis extinction spectra were recorded with a UV/Vis spectrometer (Varian, Cary 50).

In a typical procedure, samples for correlated SEM and SERS experiments were prepared by drop casting a suspension of the sample in ethanol on a Si substrate that had been patterned with registration marks and letting it dry under ambient conditions. Once the sample had dried, it was rinsed with copious amounts of ethanol, immersed in a 5 mM solution of 4-MBT (Aldrich) in ethanol for 1 h, taken out and washed with copious amounts of ethanol, and finally dried under a stream of air. All samples were used immediately for SERS measurements after preparation. The SERS spectra were recorded by using a Renishaw inVia confocal Raman spectrometer coupled to a Leica microscope with a 50× objective (numerical aperture (NA) = 0.90) in backscattering geometry. Light of wavelength 514 nm was generated with an argon laser coupled to a holographic notch filter with a grating of 1200 lines per millimeter. The backscattered Raman signals were collected on a thermoelectrically cooled (−60 °C) charge-coupled-device (CCD) detector. The scattering spectra were recorded in the range of 800–2000 cm^{-1} in one acquisition (accumulation: 30 s; power at the sample: 0.5 mW).

Received: September 18, 2009
Published online: November 26, 2009

Keywords: dimers · etching · nanoparticles · Raman scattering · silver

[1] a) Y. C. Cao, R. Jin, C. A. Mirkin, *Science* **2002**, *297*, 1536; b) A. P. Alivisatos, *Nat. Biotechnol.* **2004**, *22*, 47; c) A. L. Pyayt, B. Wiley, Y. Xia, A. Chen, L. Dalton, *Nat. Nanotechnol.* **2008**, *3*, 660; d) P. L. Stiles, J. A. Dieringer, N. L. Shah, R. P. Van Duyne, *Annu. Rev. Anal. Chem.* **2008**, *1*, 601; e) M. J. Banholzer, J. E. Millstone, C. A. Mirkin, *Chem. Soc. Rev.* **2008**, *37*, 885.

[2] a) S. Nie, S. R. Emory, *Science* **1997**, *275*, 1102; b) K. Kneipp, Y. Wang, H. Kneipp, L. T. Perelman, I. Itzkan, R. R. Dasari, M. S. Feld, *Phys. Rev. Lett.* **1997**, *78*, 1667.

[3] a) E. C. Le Ru, M. Meyer, E. Blackie, P. G. Etchegoin, *J. Raman Spectrosc.* **2008**, *39*, 1127; b) Z. Wang, S. Pan, T. D. Krauss, H. Du, L. J. Rothberg, *Proc. Natl. Acad. Sci. USA* **2003**, *100*, 8638; c) A. Otto, *J. Raman Spectrosc.* **2002**, *33*, 593.

[4] a) K. Kneipp, H. Kneipp, I. Itzkan, R. Dasari, M. Feld, *Chem. Rev.* **1999**, *99*, 2957; b) P. G. Etchegoin, E. C. Le Ru, *Phys. Chem. Chem. Phys.* **2008**, *10*, 6079.

[5] a) S. C. Glotzer, M. J. Solomon, *Nat. Mater.* **2007**, *6*, 557; b) G. M. Whitesides, B. A. Grzybowski, *Science* **2002**, *295*, 2418; c) R. Klajn, K. J. M. Bishop, M. Fialkowski, M. Paszewski, C. J. Campbell, T. P. Gray, B. A. Grzybowski, *Science* **2007**, *316*, 261; d) M. Rycenga, J. M. McLellan, Y. Xia, *Adv. Mater.* **2008**, *20*, 2416.

[6] a) A. P. Alivisatos, K. P. Johnsson, X. G. Peng, T. E. Wilson, C. J. Loweth, M. P. Bruchez, P. G. Schultz, *Nature* **1996**, *382*, 609; b) C. J. Loweth, W. B. Caldwell, X. G. Peng, A. P. Alivisatos, P. G. Schultz, *Angew. Chem.* **1999**, *111*, 1925; *Angew. Chem. Int. Ed.* **1999**, *38*, 1808; c) S. Y. Park, A. K. R. Lytton-Jean, B. Lee, S. Weigand, G. C. Schatz, C. A. Mirkin, *Nature* **2008**, *451*, 553; d) J. P. Novak, D. L. Feldheim, *J. Am. Chem. Soc.* **2000**, *122*, 3979; e) R. Sardar, T. B. Heap, J. S. Shumaker-Parry, *J. Am. Chem. Soc.* **2007**, *129*, 5356.

[7] W. Li, P. H. C. Camargo, X. Lu, Y. Xia, *Nano Lett.* **2009**, *9*, 485.

[8] a) S. H. Im, Y. T. Lee, B. J. Wiley, Y. Xia, *Angew. Chem.* **2005**, *117*, 2192; *Angew. Chem. Int. Ed.* **2005**, *44*, 2154; b) A. R. Siekkinen, J. McLellan, J. Chen, Y. Xia, *Chem. Phys. Lett.* **2006**, *432*, 491; c) S. E. Skrabalak, L. Au, X. Li, Y. Xia, *Nat. Protoc.* **2007**, *2*, 2182.

[9] a) X. Lu, L. Au, J. McLellan, Z. Li, M. Marquez, Y. Xia, *Nano Lett.* **2007**, *7*, 1764; b) C. Cobley, M. Rycenga, F. Zhou, Z. Li, Y. Xia, *J. Phys. Chem. C* **2009**, *113*, 16975.

[10] D. F. Evans, H. Wennerström, *The Colloidal Domain: Where Physics, Chemistry, Biology, and Technology Meet*, 2nd ed., Wiley, New York, **1999**, chap. 8.

[11] F. Zhou, Z. Y. Li, Y. Liu, Y. Xia, *J. Phys. Chem. C* **2008**, *112*, 20233.

[12] Y. Sun, B. Mayers, T. Herricks, Y. Xia, *Nano Lett.* **2003**, *3*, 955.

[13] a) G. Sauer, G. Brehm, S. Schneider, *J. Raman Spectrosc.* **2004**, *35*, 568; b) M. Osawa, N. Matsuda, K. Yoshii, I. Uchida, *J. Phys. Chem.* **1994**, *98*, 12702.

[14] a) K. Seo, E. Borguet, *J. Phys. Chem. C* **2007**, *111*, 6335; b) Y.-T. Tao, C.-C. Wu, J.-Y. Eu, W.-L. Lin, K.-C. Wu, C.-H. Chen, *Langmuir* **1997**, *13*, 4018.

[15] J. M. McLellan, Z. Y. Li, A. R. Siekkinen, Y. Xia, *Nano Lett.* **2007**, *7*, 1013.

